

NASA Contractor Report 181904

ICASE Report No. 89-64

ICASE

ON DAMPING MECHANISMS IN BEAMS

H. T. Banks

D. J. Inman

Contract Nos. NAS1-18107, NAS1-18605
September 1989

Institute for Computer Applications in Science and Engineering
NASA Langley Research Center
Hampton, Virginia 23665-5225

Operated by the Universities Space Research Association

NASA

National Aeronautics and
Space Administration

Langley Research Center
Hampton, Virginia 23665-5225

(NASA-CR-181904) ON DAMPING MECHANISMS IN
BEAMS Final Report (ICASE) 26 p CSCL 12A

N89-30010

Unclas
G3/64 0233942

ON DAMPING MECHANISMS IN BEAMS

*H. T. Banks*¹

Center for Control Sciences
Division of Applied Mathematics
Brown University
Providence, RI 02912

D. J. Inman

Mechanical Systems Laboratory
Department of Mechanical and Aerospace Engineering
State University of New York at Buffalo
Buffalo, New York 14260

Abstract

A partial differential equation model of a cantilevered beam with a tip mass at its free end is used to study damping in a composite. Four separate damping mechanisms consisting of air damping, strain rate damping, spatial hysteresis and time hysteresis are considered experimentally. Dynamic tests were performed to produce time histories. The time history data is then used along with an approximate model to form a sequence of least squares problems. The solution of the least squares problem yields the estimated damping coefficients. The resulting experimentally determined analytical model is compared with the time histories via numerical simulation of the dynamic response. The procedure suggested here is compared with a standard modal damping ratio model commonly used in experimental modal analysis.

¹This research was supported by the National Aeronautics and Space Administration under NASA Contract Nos. NAS1-18107 and NAS1-18605 while the first author was in residence at the Institute for Computer Applications in Science and Engineering (ICASE), NASA Langley Research Center, Hampton, VA 23665.

I. Introduction

In this paper a variety for damping mechanisms for a quasi-isotropic pultruded composite beam are examined. The approach taken here is a physical one. The beam is modeled by a partial differential equation describing the transverse vibration of a beam with tip mass. The damping mechanisms considered are all physically based as opposed to the usual modal models. In total, four possible damping mechanisms are considered, one external and three internal. They are: viscous damping (air damping); strain rate damping; spatial hysteresis; and time hysteresis.

In addition, various combinations of these mechanisms are considered. These physical damping models are incorporated into the Euler-Bernoulli beam equation, with care taken to formulate boundary conditions that are compatible with the various damping models. The resulting partial differential equation (integro partial differential equation in the case of time hysteresis damping) is approximated using cubic splines. The time histories of the measured experimental responses are then used to form a least squares fit-to-data parameter estimation problem. The mathematical arguments underlying this procedure are complete and imply convergence of a sequence of parameter estimates obtained from finite dimensional models to a set of best fit coefficients of the partial differential equation model. The least squares estimates of the various different damping parameters are then used in the partial (integro partial) differential equation to numerically simulate the response of the system. This numerically generated time response of the estimated system is then compared with the actual experimental time histories. These comparisons allow several conclusions to be drawn regarding the physical damping mechanisms present in the composite beam.

In particular it is shown that the spatial hysteresis model combined with a viscous air damping model results in the best quantitative agreement with the experimental time histories. The results also support the physically intuitive notion that air damping should play a more significant role in lower modes while internal damping plays a more significant role for higher modes. It is also shown explicitly that the proposed damping models listed above cannot be modeled with any degree of success or consistency by using standard modal damping ratios, as the traditional modal analysis approach completely masks the physics of damping mechanisms.

II. Basic Beam Model

The beam considered here is a pultruded quasi-isotropic composite beam constructed for use in the proposed space station (Wilson and Miserentino, 1986). As such, the configuration of interest is a cantilevered beam with a mass attached to the free end. The beam is constructed of a biaxial ($0^\circ/90^\circ$) fiberglass roving held in place with knitted polyester yarn with an equal volume of fibre

in both orientations. An isophthalic polyester resin system was used as the matrix. This material provides an alternative to aluminum which is lower in cost, has higher specific strength but is dynamically similar. As is illustrated here, this material also has interesting damping properties - dissimilar to those of aluminum.

The equation of motion for the flexural vibration of a beam is easily calculated from consideration of the equilibrium of forces acting on a differential segment of beam (see for instance Clough and Penzien, 1975). In this formulation, damping can easily be included by adding the appropriate force or moment to the equations of equilibrium. A partial differential equation model of the beam with general damping is of the form

$$u_{tt}(x,t) + L_1 u_t(x,t) + L_2 u(x,t) + \frac{\partial^2}{\partial x^2} \left[\frac{EI(x)}{\rho A} u_{xx}(x,t) \right] = f(x,t) \quad (1)$$

for $x \in (0, l)$, $t > 0$, subject to the appropriate boundary conditions and the initial conditions (taken to be $u = u_t = 0$ at $t = 0$). Here ρ is the linear mass density (mass per unit length) of the beam, A is the cross sectional area of the beam, $EI(x)$ is the spatial varying flexural stiffness of the beam, the subscript indicates partial differentiation with respect to the indicated variable and $u(x,t)$ is the beam displacement in the transverse direction at location x , time t . The function $u(x,t)$ is assumed to be smooth enough so that all the appropriate derivatives exist. The term $L_1 u_t(x,t) + L_2 u(x,t)$ is the focus of attention in this paper. The nature of the operator L_1 is determined by external damping mechanisms while the nature of the term $L_2 u(x,t)$ is determined by internal damping mechanisms.

The boundary conditions of interest here are those for a beam clamped at the end $x = 0$ and with a free end at $x = l$. In addition a mass of mass m_T and rotational inertia J , is attached at $x = l$. The fixed end requires that the displacement and the slope of the displacement both be zero. This yields:

$$u(0,t) = 0 \quad (2)$$

$$u_x(0,t) = 0 \quad (3)$$

The free end requires that the sum of the moments at $x = l$ and the sum of the forces acting at $x = l$ must each be zero. For the case of a tip mass at the free end, these boundary conditions become

$$EI(l)u_{xx}(l,t) = -J u_{tx}(l,t) \quad (4)$$

$$[EI(x)u_{xx}(x,t)]_x = m_T u_{tt}(l,t), \quad x = l \quad (5)$$

as long as only external damping is present.

Equations (1) - (5) describe the transverse vibration of a beam satisfying the Bernoulli-Euler assumption that the bending wave length is several times larger than the cross sectional

dimensions of the beam, and that only lower frequency excitations are applied to the beam. It is also assumed that rotary inertia of the beam, shear displacement of the beam and axial displacements are negligible.

If the tip mass is not present, the boundary conditions of equations (4) and (5) change accordingly. In addition, the nature of the damping operator L_2 will effect the boundary conditions. For the case of $L_1 = L_2 = 0$, the vibration analysis problem is very simple as is the inverse problem addressed here. The nature of the damping mechanisms drastically changes the nature of the solution to the vibration problem and hence controls the response of the beam. The following section discusses several possible choices for modeling the operator L_2 in equation (1) and hence the internal damping mechanisms in the beam.

III. Damping Models

As mentioned in the introduction, four models for the damping mechanisms are examined. Two of these are time independent proportional models lending themselves to modal expansions, the other two are nonproportional hysteretic models. Various combinations of these models are also considered.

Viscous Air Damping The most straight forward method of modeling the damping of a beam (or other object) vibrating in air is to use a viscous model with damping force assumed proportional to velocity. In this case the operator L_1 becomes

$$L_1 = \gamma I_0 \quad (6)$$

where I_0 is the identity operator and γ is the viscous damping constant of proportionality. The physical basis of this approach is a simple model of air resistance. As the beam vibrates it must displace air causing the force $\gamma u_t(x,t)$ to be applied to the beam. Mathematically, this form of damping is used because it is proportional and easily treated using the same methods of analysis used for undamped systems (see Inman, 1989, for instance). This form of damping is often called external damping.

Kelvin-Voigt Damping Kelvin-Voigt damping, or strain rate damping as it is sometimes called, is damping of the form

$$L_2 = c_d I \frac{\partial^5}{\partial x^4 \partial t} \quad (7)$$

where I is the moment of inertia and c_d is the strain rate damping coefficient. This model also satisfies a proportional damping criteria and hence is mathematically convenient. It is compatible with theoretical modal analysis and is also, along with viscous damping, widely used in finite

element modeling. This form of damping is often referred to as internal damping and represents energy dissipated by friction internal to the beam.

Unlike viscous external damping, inclusion of this form of damping affects the free end boundary conditions because it is strain dependent. The strain rate dependence results in a damping moment M_D of the form

$$M_D = c_d I(x) \frac{\partial^3 u}{\partial x^2 \partial t} \quad (8)$$

which is included in the derivation of the equation of motion (Clough and Penzien, 1975) and hence must also be included in any boundary conditions (such as a free end condition) depending on the moment.

The full equation of motion and boundary conditions for the case including linear viscous external damping and Kelvin-Voigt internal damping can thus be written

$$\begin{aligned} \rho u_{tt}(x,t) + \frac{\partial^2}{\partial x^2} [EIu_{xx}(x,t) + c_d Iu_{xxt}(x,t)] + \gamma u_t(x,t) &= f(x,t), \quad x \in (0,l), \quad t > 0 \\ u(0,t) = u_x(0,t) &= 0, \quad t > 0 \\ EIu_{xx}(l,t) + c_d I u_{xxt}(l,t) &= -J u_{xt}(l,t), \quad t > 0 \\ \frac{\partial}{\partial x} [EIu_{xx}(x,t) + c_d Iu_{xxt}(x,t)] &= m_T u_{tt}(x,t), \quad x = l, \quad t > 0. \end{aligned} \quad (9)$$

Here, note that the tip mass as well as the damping moment are represented in the boundary conditions. The total damping mechanism used in (9) is the analog to proportional damping (i.e., a linear combination of mass and stiffness operators).

Time Hysteresis Hysteretic damping terms are most commonly associated with sinusoidal loadings. The generic idea of including a mechanism in the beam vibration constitutive equation indicating that stress is proportional to strain plus the past history of the strain can be accomplished by introducing an integral term of the form

$$\int_{-r}^0 g(s) u_{xx}(x,t+s) ds \quad (10)$$

with the history kernel $g(s)$ defined by

$$g(s) = \frac{\alpha e^{\beta s}}{\sqrt{-s}} \quad (11)$$

where α and β are constants. Since the introduction of the heredity integral occurs in the stress strain relationship, the boundary conditions must also be modified. In this case the boundary value problem of interest becomes

$$\rho u_{tt}(x,t) + \frac{\partial^2}{\partial x^2} \left[EI u_{xx}(x,t) - \int_{-r}^0 g(s) u_{xx}(x,t+s) ds \right] = f(x,t), \quad x \in (0,1), \quad t > 0$$

$$u(0,t) = u_x(0,t) = 0 \quad t > 0 \quad (12)$$

$$EI u_{xx}(l,t) - \int_{-r}^0 g(s) u_{xx}(l,t+s) ds = J u_{xll}(l,t), \quad t > 0$$

$$\frac{\partial}{\partial x} \left[EI u_{xx}(x,t) - \int_{-r}^0 g(s) u_{xx}(x,t+s) ds \right] = m_T u_{tt}(x,t), \quad x = l, \quad t > 0$$

It is emphasized again that the inclusion of a damping moment in the equation of motion also affects the boundary condition.

Spatial Hysteresis Another type of damping (proposed by Russell, 1990) is based on interpreting the energy lost in the transverse vibration of a beam as resulting from differential rates of rotation of neighboring beam sections causing internal friction. This can be modeled by the damping expression

$$\frac{\partial}{\partial x} \left[\int_0^l h(x,\xi) \{ u_{xt}(t,x) - u_{xt}(t,\xi) \} d\xi \right] \quad (13)$$

where the kernel $h(x,\xi)$ may be defined, for example, by

$$h(x,\xi) = \frac{a}{b\sqrt{2\pi}} e^{-(x-\xi)^2/2b^2}. \quad (14)$$

Under these circumstances the model for the beam vibration becomes (including viscous external damping)

$$\rho u_{tt}(x,t) + \frac{\partial^2}{\partial x^2} [EI u_{xx}(x,t)] + \gamma u_t(x,t)$$

$$- \frac{\partial}{\partial x} \left[\int_0^l h(x,\xi) \{ u_{xt}(x,t) - u_{xt}(\xi,t) \} d\xi \right] = f(x,t), \quad x \in (0,l), \quad t > 0 \quad (15)$$

$$u(0,t) = u_x(0,t) = 0, \quad t > 0$$

$$EI u_{xx}(l,t) = -J u_{xll}(l,t) \quad t > 0$$

$$\frac{\partial}{\partial x} [EIu_{xx}(x,t)] - \left[\int_0^l h(x,\xi) \{u_{xt}(x,t) - u_{xt}(\xi,t)\} dx \right] = m_T u_{tt}(x,t), \quad t > 0, x = l$$

where again the internal damping mechanism is reflected in the boundary conditions.

In total, the models described by systems (9), (12) and (15) represent four possible mechanisms of damping taken in various combinations. The approach taken here is to attempt to fit each of the combinations of damping models listed above to experimentally measured data. By examining each model's numerical solution in comparison with measured data, a best model is chosen from these as being most representative of the cantilevered quasi-isotropic beam. As is discussed in Section V, these models all admit reasonable mathematical treatment.

IV. Problem Statement

The various damping coefficients introduced in the preceding discussion cannot be measured by static experiments. Thus, the damping constants γ , c_d , α , β , a , and b must all be estimated based on measurements taken from dynamic experiments. The procedure suggested here is to estimate various groups of damping parameters such as indicated in the three models of (9), (12) and (15). Once these coefficients are estimated they can be used in the model to produce a numerical simulation of the response of the structure under consideration subjected to identical experimental inputs. The analytical time response (with the estimated coefficients) is then compared to the experimentally measured time response. The model that best agrees with (predicts) the experimental response is then considered to be a valid and desirable physical model.

In particular, several vectors of parameters \mathbf{q} are defined, one for each model of interest. For the three cases discussed here they are:

$$\mathbf{q}_1 = [EI, c_d I, \gamma] \quad (16)$$

which delineates the first damping model as defined by system (9). Here c_d is the internal strain rate damping coefficient and γ is the linear air damping coefficient. The second model considered, as defined by system (12), is characterized by the parameter vector

$$\mathbf{q}_2 = [EI, \alpha, \beta] \quad (17)$$

where α and β characterize the time hystoretic damping term. The last model considered contains a combination of linear air damping, defined by the coefficient γ , and spatial hysteresis defined by the constants a and b . The parameter vector for the third system defined by (15) is

$$\mathbf{q}_3 = [EI, \gamma, a, b]. \quad (18)$$

Other combinations of the four damping mechanisms were considered but were dismissed as discussed in the later section on results. Even though the techniques (Spline Inverse Procedures) described below can readily be used to treat spatially varying coefficients EI and $c_d I$, the experiments for the efforts presented in this paper were performed on uniform beams. Hence, consideration in this paper will hence forth be restricted to constant EI and $c_d I$.

Note that in each case the parameter vector contains the flexural stiffness constant EI . For most common materials EI is tested, tabulated and well known. However in this case the material is a prototype composite with unknown material properties. Thus EI is also estimated. Because of the relative size of the air damping coefficient c_d , the term $c_d I$ is estimated.

V. Mathematical Foundation of the Estimation Problem

Two approaches to solving the problem of determining the coefficients in the vectors \mathbf{q}_1 , \mathbf{q}_2 and \mathbf{q}_3 are formulated here. The first approach involves application of experimental modal analysis methods (see Ewins, 1988 or Inman, 1989) to a theoretical modal analysis of equation (1). This procedure, suggested by Clough and Penzien (1975), can only be applied to the problem of estimating \mathbf{q}_1 because modal analysis is not applicable to the hysteresis terms in \mathbf{q}_2 and \mathbf{q}_3 . This modal approach is presented for comparison and because it represents a standard approach for measuring damping. However, modal approaches cannot be used to solve the inverse problem for general constitutive elements. The inverse procedures suggested as the second approach here do not have this limitation and can be applied to systems with spatially dependent physical parameters (EI , etc.) as well as exotic damping mechanisms.

The second approach taken here is a nonmodal procedure applicable to all three estimation problems, and forms our proposed method. This method is based on a careful consideration of the distributed parameter nature of the test article. It consists of forming a sequence of finite dimensional approximations (Galerkin type cubic B -splines) to equation (1) with an associated least squares fit-to-data (see Banks and Kunisch, 1989, for a general discussion of these ideas). For each of the damping models presented in this paper, a corresponding sequence of approximate estimates \mathbf{q}_i^N can be shown to converge to a best-fit parameter \mathbf{q}_i for the original distributed parameter system (1) (or specifically for (9), (12), or (15)). Detailed convergence arguments are given in Banks et al (1983, 1986, 1988, 1989), Banks and Ito (1988). The computational algorithms proposed here are based on these considerations of the distributed parameter nature of the estimation problem and is called the Spline-based Inverse Procedure (SIP).

Modal Analysis (EMA) The typical experimental approach to measuring the damping in a structure is to use experimental modal analysis (EMA) to determine modal damping ratios and natural frequencies. These quantities can then be used to determine the physical parameters contained in the vector \mathbf{q}_1 . In the case discussed here, the tip mass is removed (for ease in exposition) so that $m_T = J = 0$, and the unit interval is used (i.e., $l = 1$). The damping operators L_1 and L_2 become

$$L_1 = \frac{\gamma}{\rho A} \quad , \quad L_2 = \frac{c_d I}{\rho A} \frac{\partial^5}{\partial x^4 \partial t} \quad (19)$$

which commute with the stiffness operator so that a modal representation is possible (Caughey and O'Kelley, 1965). According to this theory (see for instance Inman, 1989) the solution of (9) can be written as a series of products of two functions, $u_m(x,t) = a_m(t) \phi_m(x)$, which satisfy (9) for each m and whose sequence of partial sums converges to the unique solution of (9). Here the normalized functions $\phi_m(x)$ are the eigenfunctions (mode shapes) of the stiffness operator

$$\frac{\partial^2}{\partial x^2} \left(\frac{EI}{\rho A} \frac{\partial^2}{\partial x^2} \right) \quad (20)$$

subject to the boundary conditions of system (9). These eigenfunctions satisfy (for EI constant)

$$\frac{\partial^4}{\partial x^4} \phi_m(x) = \beta_m^4 \phi_m(x) \quad (21)$$

where $\beta_m^4 = \omega_m^4 (\rho A / EI)^2$ and the ϕ_m satisfy the orthogonality condition

$$\int_0^1 \phi_n(x) \phi_m(x) dx = \delta_{nm} \quad (22)$$

Here δ_{nm} is the Kronecker delta and ω_m are the undamped natural frequencies of the system.

Substituting $u_m(x,t)$ into equation (1), multiplying by $\phi_m(x)$ and integrating with respect to x over the interval (0,1), one finds that each $a_m(t)$ must satisfy

$$\ddot{a}_m(t) + \left(\frac{\gamma}{\rho A} + \frac{c_d I}{\rho A} \beta_m^4 \right) \dot{a}_m(t) + \frac{EI}{\rho A} \beta_m^4 a_m(t) = \int_0^1 f(x,t) \phi_m(x) dx, \quad t > 0 \quad (23)$$

for all $m = 1, 2, 3, \dots$. Equation (23) has a direct relationship to the frequency domain measured modal data available from EMA. The experimental modal analysis procedure assumes that the structure consist of some finite number of single degree of freedom oscillators of the form:

$$\ddot{a}_m(t) + 2\zeta_m \hat{\omega}_m \dot{a}_m(t) + \omega_m^2 a_m(t) = f_m \quad (24)$$

where $\hat{\zeta}_m$ and $\hat{\omega}_m$ are measured damping ratios and natural frequencies respectively. Comparing coefficients of a_m and \dot{a}_m in equations (23) and (24), one obtains

$$\beta_m^4 \frac{EI}{\rho A} = \hat{\omega}_m^2 \quad (25)$$

and

$$\frac{\gamma}{\rho A} + \frac{c_d I}{\rho A} \beta_m^4 = 2 \hat{\zeta}_m \hat{\omega}_m \quad (26)$$

for each m .

As outlined in Cudney and Inman (1989), the elastic modulus E may be estimated from equation (25) by a linear least squares fit by which one obtains

$$E = \frac{1}{K} \sum_{m=1}^K \frac{4\pi^2 \rho A}{I \beta_m^4} \hat{f}_m^2 \quad (27)$$

where $\hat{f}_m = \hat{\omega}_m / 2\pi$ hertz with $(\hat{\zeta}_m, \hat{\omega}_m)$, $m = 1, 2, \dots, K$, a given measured set. Equation (26) can be written down once for each pair in this measured set $(\hat{\zeta}_m, \hat{\omega}_m)$, $m = 1, 2, \dots, K$, to produce a least squares determination of the damping parameters of the form

$$\begin{bmatrix} \gamma \\ c_d \end{bmatrix} = B^\dagger \mathbf{z}. \quad (28)$$

Here B^\dagger denotes the generalized inverse (least square) of the $2 \times K$ matrix

$$B = \frac{1}{\rho A} \begin{bmatrix} 1 & \beta_1^4 I \\ 1 & \beta_2^4 I \\ \vdots & \vdots \\ \vdots & \vdots \\ 1 & \beta_K^4 I \end{bmatrix} \quad (29)$$

and \mathbf{z} is the $K \times 1$ vector $\mathbf{z} = [2 \hat{\zeta}_1 \hat{\omega}_1, 2 \hat{\zeta}_2 \hat{\omega}_2, \dots, 2 \hat{\zeta}_K \hat{\omega}_K]^T$ of measured modal information. The entries in B are calculated from the analytical solution of the eigenvalue problem for the stiffness operator above with appropriate boundary conditions.

Equation (28) (and/or a weighted version of it) can be used to estimate the distributed damping parameters for the problem involving \mathbf{q}_1 . While intuitively obvious and straight forward, this modal based method requires that EI must be constant and that β_m must be known in closed form. In addition, this approach is not applicable to the noncommuting damping models involving \mathbf{q}_2

and \mathbf{q}_3 or to problems with spatially varying coefficients. This provides the motivation for the nonmodal approach developed next.

Spline Inverse Procedure (SIP) An alternative to estimating \mathbf{q}_i from measured modal data (frequency domain) is to formulate a parameter estimation problem based on measured time histories of the test structure's response. Let $\hat{u}_{tt}(l, t_i)$ denote the acceleration measurements at the tip of the beam ($x = l$) at various times t_i . The inverse problem of interest is then to find the vector of parameters \mathbf{q} such that

$$J(\mathbf{q}) = \sum_{i=1}^M |u_{tt}(l, t_i, \mathbf{q}) - \hat{u}_{tt}(l, t_i)|^2 \quad (30)$$

is minimized where $u(x, t, \mathbf{q})$ denotes the solution of equation (1) with the appropriate boundary and initial conditions corresponding to parameter values \mathbf{q} . Here M is the number of tip acceleration measurements.

This estimation problem cannot, of course, be solved analytically. However, an iterative optimization scheme coupled with an approximation method for the infinite dimensional system of equation (1) may be used. The procedure suggested here is outlined as follows. First equation (1) is approximated via Galerkin procedures using cubic spline elements (N is used to denote the approximation index) to yield an approximate finite dimensional version which is solved for $u^N(t)$. The approximate accelerations u_{tt}^N are then used in the cost function of equation (30) to define the finite dimensional estimation problem of minimizing

$$J^N(\mathbf{q}) = \sum_{i=1}^M |u_{tt}^N(l, t_i, \mathbf{q}) - \hat{u}_{tt}(l, t_i)|^2. \quad (31)$$

The solution of this set of estimation problems yields a sequence of estimates, denoted $\{\mathbf{q}^N\}$, of best fit parameters. Under appropriate assumptions, this sequence is then shown to converge to \mathbf{q}^* , a vector of parameters for the fully distributed parameter model of equation (1) which minimizes $J(\mathbf{q})$ of equation (30). The theoretical formulation of this approach is presented next. The required proofs are omitted but can be found in Banks and Ito (1988), Banks, et al (1983, 1986, 1989), and Banks and Kunisch (1989).

The SIP estimation algorithm is formulated in weak or variational form by multiplying equation (1) by $\psi(x)$ and integrating over in the interval $(0, l)$. This yields

$$\langle u_{tt}, \psi \rangle + \langle L_1 u_t, \psi \rangle + \langle L_2 u, \psi \rangle = \langle f, \psi \rangle \quad (32)$$

where the inner product $\langle \cdot, \cdot \rangle$ for the Hilbert space $H = L_2(0, l)$ is defined by

$$\langle \phi_1, \phi_2 \rangle = \int_0^l \phi_1(x)\phi_2(x)dx . \quad (33)$$

Equation (32) must hold for all ψ in V , a Hilbert space continuously and densely imbedded in the Hilbert space H , containing the solution of (1) subject to the appropriate boundary conditions. (In this case $V = \{\psi \in H^2(0,l): \psi(0) = \psi'(0) = 0\}$ where H^2 is the Sobolev space of functions possessing first and second derivatives in $L_2(0,l)$). The terms in equation (32) are now identified with elements $\ddot{u}(t;\mathbf{q})$, $\dot{u}(t;\mathbf{q})$ and $u(t;\mathbf{q})$ which evolve in time, and satisfy (in a generalized or weak sense - see Banks and Ito (1988) and Banks and Kunisch (1989)) the evolution equation

$$\ddot{u}(t;\mathbf{q}) + \mathbf{B}(\mathbf{q}) \dot{u}(t;\mathbf{q}) + \mathcal{A}(\mathbf{q}) u(t;\mathbf{q}) = f(t), \quad t > 0 \quad (34)$$

subject to the appropriate initial conditions. Here the explicit dependence on the parameter vector \mathbf{q} is emphasized, while the solution of equation (34) is a function of time for each x (or, alternatively, is thought of as a function of x for each t , the function being an element of V for each t). The operators \mathcal{A} and \mathbf{B} can be appropriately defined using the corresponding terms in (32).

The Galerkin approach employing cubic spline subspaces to solve (34) (or equivalently (32)) iteratively is explained next. Given a value of N and a vector \mathbf{q} , an approximate solution to (34) in $X^N = \text{span} \{B_0^N, \dots, B_N^N\}$ is sought of the form

$$u^N(t;\mathbf{q}) = \sum_{j=0}^N w_j^N(t) B_j^N = \sum_{j=0}^N w_j^N(t;\mathbf{q}) B_j^N \quad (35)$$

where $\{B_j^N\}$ is the set of cubic spline basis functions appropriately modified to be in the domain of definition of the operators in equation (34). More precisely, let $\Delta^N = \{x_i\}_{i=0}^N$ with $x_i = il/N$ for $i = 0, 1, \dots, N$, and let $\tilde{B}_j^N, j = -1, \dots, N+1$ denote the standard $C^2(0,l)$ basis elements for the cubic B -spline subspaces of dimension $N+3$ corresponding to the grid Δ^N (see Prenter, 1975). Here $C^2(0,l)$ is the set of all continuous functions with continuous first and second derivatives on the interval $(0,l)$. Then B_j^N is given by

$$B_j^N = \tilde{B}_j^N, \quad \text{for } 2 < j < N-2$$

$$B_0^N = \tilde{B}_0^N - 4 \tilde{B}_{-1}^N, \quad B_N^N = \tilde{B}_N^N - 4 \tilde{B}_{N+1}^N$$

$$B_1^N = \tilde{B}_0^N - 4 \tilde{B}_{-1}^N, \quad B_{N-1}^N = \tilde{B}_N^N - 4 \tilde{B}_{-1}^N.$$

Note then that $X^N = S_0^3(\Delta^N) = \{\phi \in S^3(\Delta^N): \phi(0) = \phi(l) = 0\}$ where $S^3(\Delta^N) = \{\phi \in C^2(0,l); \phi \text{ is a cubic polynomial on each interval } [x_i, x_{i+1}]\}$.

The approximate solutions to (34) are determined from requiring that for all functions $z \in X^N$

$$\langle \ddot{u}^N(t), z \rangle + \langle \mathfrak{B}(q) \dot{u}^N(t), z \rangle + \langle \mathcal{A}(q) u^N(t), z \rangle = \langle f(t), z \rangle \quad (36)$$

with appropriate projected initial condition. Choosing $z = B_i^N$ and using equation (35) one may write this in an equivalent matrix form as

$$\ddot{\mathbf{w}}^N(t) + D^N \dot{\mathbf{w}}^N(t) + K^N \mathbf{w}^N(t) = \mathbf{F}^N(t) \quad (37)$$

where \mathbf{w}^N is the $N+1 \times 1$ vector $[w_0^N, w_1^N, \dots, w_N^N]^T$ and where the $N+1 \times N+1$ "damping" and "stiffness" matrices D^N and K^N are defined by

$$D_{ij}^N = \langle B_i^N, \mathfrak{B}(q) B_j^N \rangle$$

$$K_{ij}^N = \langle B_i^N, \mathcal{A}(q) B_j^N \rangle$$

Here the subscript ij denotes the ij^{th} element of the matrix and the vector \mathbf{F}^N is defined as the $N \times 1$ vector of elements $F_j^N = \langle f(t), B_j^N \rangle$. Each approximate identification problem now reduces to calculating \mathbf{q}^N that minimizes (31) subject to the vector differential equation (37). These calculations result in the sequence $\{\mathbf{q}^N\}$ which, as mentioned above, converges to a \mathbf{q} minimizing (30) subject to systems (9), (12) or (15), as appropriate.

It is important to note here that this approximation differs from a standard finite element methods in two fundamental ways. First, the damping mechanism produced by the matrix D^N converges to a physical damping model. Typical finite element models treat damping in an ad hoc fashion. Secondly, the entire model converges to a strength of materials/continuum mechanics model

having more physical significance than the rather arbitrary node model produced by standard finite element approximations.

VI. Test Procedures

This section describes a series of experiments performed to examine the proposed damping mechanisms and validate the approach (SIP) proposed in this paper. Figure 1 is a schematic of the experimental configuration. The experiments were performed in the Mechanical Systems Laboratory at the State University of New York at Buffalo. The beam is set up in a cantilevered arrangement with a removable and adjustable tip mass. The geometric properties of the beam are listed in Table 1.

Substantial effort was made to insure that the fixed end behaved as a true clamped boundary condition. The clamp consisted of a large iron mass held together with a very strong magnetic field. The beam was extended an equal length beyond the clamp. The motion of the clamp and the extended portion of the beam were monitored to insure that no energy was lost to motion of the clamp and that no motion was transmitted through the clamp to the extended beam. The theoretical values of β_n for a clamp-free beam (i.e., the solution to the transcendental characteristic equation) are listed in Table 2 for reference.

The beam was excited by hammer hits. The hammer used was a Kistler Instrument Company (KIC) model with a load cell at its tip which allows a measurement of the input force. The tip of the hammer has variable mass and stiffness to insure excitation of the beam in the frequency range of interest. The hammer's load cell signal was run through a signal conditioning device (KIC) to the input channel of a GENRAD 2515 data acquisition and analyzer system for processing.

It should be noted that many experimentalists suggest using a shaker along with swept sine or random excitation so that time histories of the forcing functions are repeatable in subsequent tests. However, because of the flexible nature of the structure (the first mode natural frequency is 3.64 Hz) it was observed that attaching shaker to the structure either at the root or near the tip of the beam altered the measured natural frequencies. Consequently impact tests were used with the exception that the first mode was confirmed by analyzing the free response of the beam to an initial deflection in the first mode shape.

The beam response was measured by using KIC piezobeam accelerometers and associated signal conditioning as well as a laser vibrometer (DISA), which provides a direct velocity measurement and a check on the accelerometer signals. The output responses are fed to the remaining channels

of the GENRAD analyzer. Once the response signals are in the analyzer they are digitized and stored for various programs written to perform the above analyses.

In the modal analysis approach, the digital records of the input and output signals were manipulated into transfer functions and analyzed in the frequency domain using the Nyquist circle fit method (see Ewins 1984, for instance). The computed modal data $\hat{\zeta}_m$ and $\hat{\omega}_m$ was averaged at least 15 times for each mode. The EMA program used was a standard commercially available EMA package (SDRC) and the results were checked using several other standard frequency domain algorithms.

One popular alternative to frequency domain EMA is to use time domain realization methods. This approach uses the digitized time histories to construct a finite dimensional state matrix for the test structure. The numerical solution of the eigenvalue problem for this state matrix then yields the desired modal constants $\hat{\zeta}_m$ and $\hat{\omega}_m$. One algorithm for this is the Eigensystem Realization Algorithm (ERA) developed at NASA by Juang and Pappa (1985). Data from the analyzer was transported by direct link to a VAX 11785 containing ERA. The results obtained by this approach agreed with those of the Nyquist approach lending credibility to the measured modal data.

The experimentally determined modal data was then down loaded to a commercial matrix computation package (Moler et al 1987) where various least squares algorithms were used to solve equation (28) for the desired distributed parameters γ and c_d .

The time domain test data was also sent via BITNET to Brown's IBM 3090. The above described SIP methodology was applied to this data and q_1 , q_2 and q_3 estimated. Several tests were run in various configurations to investigate the effects of various tip mass arrangements as well as to examine various combinations of damping mechanisms. A large number of tests were performed over a two year period; in the following section, the findings of these tests are summarized.

VII. Results

The results of estimating the various damping parameters using EMA are discussed first as it is limited to the problem defined by q_1 . In the EMA approach, the correctness of a given estimate is judged by the ability of the solution to produce frequency independent parameters γ and c_d . Next, the results of the SIP approach are used to examine the damping mechanism. In this case the success of a given estimate is judged on the ability of the estimate to numerically simulate the experimental time history of the structure's response.

Experimental Modal Analysis The results of performing 15 modal tests, as outlined in Section VI, are listed in Table 3, for the system without a tip mass. Note the large damping ratios exhibited by this material when compared with calculated values of aluminum or steel. This data was first used in equation (27) to determine the values of the modulus (E) calculated to be

$$E = 2.68 \times 10^{10} \text{ N/m}^2 \quad (38)$$

with a variance of 0.6 N/m^2 .

The excellent fit provided by the Bernoulli-Euler beam stiffness to the measured frequencies indicates that this is a suitable stiffness model for this particular composite with $0^\circ/90^\circ$ orientations. Some researchers have suggested that a Timoshenko model might be more appropriate for composites. However the inclusion of rotary inertia and shear effects did not provide a convincing fit to the data obtained here.

It has been shown by Cudney and Inman (1988) that attempting to use just air damping, γ , or just strain rate damping, c_d , alone fails to match the measured modal data. In each case the attempt to fit a single damping parameter is measured by the ability of the estimated values of γ and c_d , to reproduce the measured damping ratios $\hat{\zeta}_m$. This situation is discussed later in the context of the SIP estimates. The significance of this result is that a single modal damping ratio cannot logically be used to model the damping mechanism of the composite beam.

Next the generalized inverse of the data matrix B defined by equation (29) and the theoretical values of the eigenvalues given in Table 2 are used to calculate the desired damping coefficients γ and c_d from equation (28) and the vector z . The vector z contains the experimentally determined modal data of Table 3. The results of γ and c_d are

$$\gamma = 1.7561 \text{ N-sec/m}^2, \quad c_d = 2.05 \times 10^5 \text{ N-sec/m}^2 \quad (39)$$

for 9 modes of data.

The effect of natural frequency on the measured modal damping ratio $\hat{\zeta}_m$ is seen by substituting the analytical expression for β_m into equation (26). This yields that

$$\hat{\zeta}_m = \frac{\gamma}{2\hat{\omega}_m} + \frac{c_d}{2E^2I} \hat{\omega}_m. \quad (40)$$

This indicates clearly that the effect of air damping (8) decreases with increasing mode number ($\hat{\omega}_m \rightarrow \infty$). Thus for higher modes the strain rate damping makes a more significant contribution to the measured damping ratio. This agrees with the physically intuitive notion that the low

frequency modes are pushing more air than the higher frequency lower amplitude modes. In fact, for a free-free configuration it is claimed by Vinson (1989) that the effect of air damping can be subtracted based on Blevins' equation (Blevins, 1977) which considers flow effects.

To check the validity of this model, the frequency dependence of the coefficients γ and c_d was examined by recalculating them using a different number of modes. Successive least squares was performed using first 2 modes, then 3 modes, etc., up to the total of 9 modes. The result is illustrated in Table 4. Table 4 indicates that the estimates of γ and c_d depend somewhat on the frequency range of interest. This is inconsistent with the physical models put forth in Section III for estimating \mathbf{q}_1 . Furthermore this approach is not applicable to the problem of estimating \mathbf{q}_2 and \mathbf{q}_3 . Hence, one must conclude that the modal approach is not satisfactory in attempting to model, in composite beams, any of the damping mechanisms proposed in this paper.

Spline Inverse Procedure The use of the SIP provides a nonmodal approach appropriate for each of the problems of estimating \mathbf{q}_1 , \mathbf{q}_2 and \mathbf{q}_3 . The problem of estimating \mathbf{q}_1 is solved first for comparison with the modal approach. This problem was solved again using a slightly more complicated cantilevered beam with a tip mass. The stiffness parameter (elastic modulus) E was estimated to be $2.71 \times 10^{10} \text{N/m}^2$, in good agreement with the modal estimation results above. Estimates of air damping alone or strain rate alone as a damping model proved to be inadequate in reproducing time histories matching those of the experimental data, indicating a poor model. This is again in agreement with the results obtained by using the modal approach.

The time domain approach provided by SIP allows a convenient comparison between the measured time response and the analytical time response generated by the model of equation (9) with the experimentally determined parameter vector \mathbf{q}_1 . The difference between the numerical solution for the time history of the acceleration $u_{ii}(x_i, t)$ for the analytical model with the estimated parameter \mathbf{q}_1 and the experimentally measured accelerations define the residual which is generally small (Banks et al., 1987). The analytical time response is plotted along with the measured time response versus time in Figure 2. While the agreement is fair, the residual is larger for longer time intervals, warranting further modeling.

Next the temporal hysteresis model involving \mathbf{q}_2 was considered as a possible candidate for modeling the damping in the composite. In this case, the estimation procedure produces (i.e., consistent with our previous methods for estimating \mathbf{q}_1) a good value for E but drives the air damping coefficient to zero. The residual, however, is better than that for the model with \mathbf{q}_1 . Figure 3 illustrates a plot of the measured acceleration versus time as well as the acceleration

predicted by the model with the estimate q_2 . The difference between the measured and predicted value over the time interval of interest is almost negligible. Because this model drives the air damping coefficient to zero (violating physical intuition), a third model (q_3) was considered.

The last model considered is based on a concept of spatial hysteresis as defined by the estimation problem for q_3 . Again the resulting estimate of the elastic modulus E is consistent with those estimated previously. The values estimated for the spatial hysteresis parameters ($a = 1.040394$, $b = 0.064362$) and an air damping coefficient ($\gamma = .090189$) produce an excellent match between predicted and measured response as indicated in Figure 4 (Banks, et al. 1988). However, the external damping coefficient γ differs from that estimated using the parameter vector q_1 ($\gamma = .0315$) emphasizing the fact that air damping should not be estimated independently whenever internal damping mechanisms are present.

VIII. Conclusion and Discussion

Three different models of damping have been presented to account for the experimentally observed dissipation in a pultruded composite beam. A spline based inverse procedure (SIP) which relies on the distributed parameter nature of the damping mass and stiffness parameters was proposed and used to estimate the form of each damping mechanism. External air damping, strain rate damping, spatial hysteresis and time hysteresis models were considered. The spline based method was also compared to a standard experimental modal analysis (EMA) approach. The EMA approach is not applicable to the various hysteresis models, nor is it applicable to systems with spatially varying parameters in general. Both the SIP and EMA approaches yield consistent values for the elastic modulus (E) for all three estimation models. This is consistent with the fact that frequencies are much more robust to estimates than are damping quantities.

Both hysteresis models produce better results than the strain rate damping model. However, the spatial hysteresis model allows for the air damping term while time hysteresis does not. Since air damping is obviously present, the time hysteresis result is less satisfying. A comparison of the hysteresis models is given in Banks, et al (1988). As indicated in that presentation further analysis and modeling is required before a conclusive decision can be made about a best model. It is clear from the results presented here that hysteretic damping is able to reproduce experimental time responses with more accuracy than the standard Kelvin-Voigt model. It is also clear that the standard method of measuring damping, EMA, does not provide an accurate method for investigating the energy dissipation in the composite beam tested here.

In summary, a new method of determining damping mechanisms in a distributed parameter model has been proposed and applied to a beam. The method referred to as SIP, also yields estimates of the stiffness parameters. This method has been compared to the standard method of determining damping in structures using modal methods. When compared on the same experimental test data, the SIP approach produces more consistent estimates of the Kelvin-Voigt damping parameter than those obtained by using modal methods. In addition, the proposed procedure is applicable to hysteretic damping models and to systems with spatially varying parameters that cannot be treated by modal methods.

IX. Acknowledgements

This research was supported in part under the following grants and contracts: NASA: NAG-1-517 (HTB) and NAG-1-785 (DJI); NSF: MSM-8351807 (DJI) and MCS-8504316 (HTB); AFOSR: F49620-86-C-0111 (HTB and DJI) and several DOD equipment grants: AFOSR: 85-0119,87-0099 (DJI). The authors also wish to acknowledge H.H. Cudney, R.H. Fabiano and Y. Wang for numerous discussions and for their efforts on both the experimental and computational aspects of this project.

X. References

- Banks, H.T., Crowley, J.M. and Kunisch, K., 1983, "Cubic Spline Approximation Techniques for Parameter Estimation in Distributed Systems," *IEEE Transactions on Automatic Control*, Vol. AC-28, No. 7, pp. 773-786.
- Banks, H.T., Crowley, J.M. and Rosen, I.G., 1986, "Methods for the Identification of Material Parameters in Distributed Models for Flexible Structures," *Mat. Aplicada e Comput.*, Vol. 5, pp. 139-168.
- Banks, H.T., Fabiano, R.H., Wang, Y., Inman, D.J. and Cudney, H.H., 1988, "Spatial Versus Time Hysteresis in Damping Mechanisms," *Proceedings of the 27th IEEE Conference on Decision and Control*, pp. 1674-1677.
- Banks, H.T., Fabiano, R.H. and Wang, Y., 1989, "Inverse Problem Techniques for Beams with Tip Body and Time Hysteresis Damping," *Mat. Aplicada e Comput.*, to appear.
- Banks, H.T. and Ito, K., 1988, "A Unified Framework for Approximation and Inverse Problems for Distributed Parameter Systems," *Control, Theory and Advanced Technology*, Vol. 4, pp. 73-90.

Banks, H.T. and Kunisch, K., 1989, *Estimation Techniques for Distributed Parameter Systems*, Birkhäuser, Boston, MA

Banks, H.T., Wang, Y., Inman, D.J. and Cudney, H.H., 1987, "Parameter Identification Techniques for the Estimation of Damping in Flexible Structures Experiments," Proceedings of the 26th IEEE Conference on Decision and Control, Vol. 2, pp. 1392-1395.

Blevins, R.D., 1977, *Flow-Induced Vibration*, Van Nostrand Reinhold, New York.

Caughey, T.K. and O'Kelly, M.E.J., 1965, "Classical Normal Modes in Damped Linear Systems," *ASME Journal of Applied Mechanics*, Vol. 37, pp. 583-588.

Clough, R.W. and Penzien, J., 1975, *Dynamics of Structures*, John Wiley and Sons, New York, NY, 1975.

Cudney, H.H. and Inman, D.J., 1989, "Experimental Verification of Damping Mechanisms in a Composite Beam," Proceedings of the 7th International Modal Analysis Conference, pp. 904-910.

Ewins, D.J., 1988, *Modal Testing Theory and Practice*, Research Studies Press, Letchworth, England.

Inman, D.J., 1989, *Vibration with Control, Measurement and Stability*, Prentice Hall, Englewood Cliffs, NJ.

Juang, J.-N. and Pappa, R.S., 1985, "An Eigensystem Realization Algorithm for Modal Parameter Identification and Model Reduction," *AIAA Journal of Guidance, Control and Dynamics*, Vol. 8, No. 5, pp. 620-627.

Moler, C., Little, J. and Bangert, S., 1987, *PC-MATLAB Users Guide*, The Mathworks, Inc.

Prenter, P.M., 1975, *Splines and Variational Methods*, Wiley-Interscience, New York.

Russell, D.L., 1990, "On Mathematical Models for the Elastic Beam with Frequency Proportional Damping," *Control and Estimation in Distributed Parameter Systems*, SIAM.

Spirnak, G.T. and Vinson, J.R., 1988, "The Effect of Temperature on the Material Damping of Graphite; Epoxy Composites in a Simulated Space Environment," *Recent Advances in the Macro-Micro-Mechanics of Composite Materials and Structures*, AD- Vol. 4, ASME, pp. 189-192.

Wilson, M.L. and Miserentino, R., 1986, "Pultrusion Processes Development for Long Space Boom Models," Proceedings of the 41st Annual Conference of the Reinforced Plastics/Composites Industry, Paper #6-D.

Table 1. Beam parameters.

Length (meters) (l)	1.0
Moment of Inertia (meter ⁴) (I)	1.64 x 10 ⁻⁹
Density (kilograms/meter ³) (ρ)	1710
Area, cross section (meter ²) (A)	0.597 x 10 ⁻³

Table 2. Theoretical eigenvalues of a clamped-free beam.

Mode Number	Eigenvalue (β_i)
1	1.875
2	4.694
3	7.855
4	10.996
5	14.137
6	17.279
7	20.420
8	23.562
9	26.704

Table 3. Experimentally measured modal data.

Mode	Theoretical Freq. (Hz.)	Experimental Freq. (Hz.)	Damping Ratio (%)	Std. Dev.
2	23.096	22.8	.218	.015
3	64.675	65.3	.227	.016
4	126.740	127	.154	.003
5	209.488	212	.228	.023
6	312.955	314	.120	.008
7	437.075	435	.131	.021
8	581.475	580	.155	.010
9	747.475	733	.202	.015

Table 4. Estimates of damping based on using a successive number of nodes (all values in N sec/m²).

Modes	Viscous Only	Strain Only	Viscous and Strain	
	C_1	$C_d, \times 10^6$	C_1	$C_d, \times 10^6$
1-2	.3619	.8024	.0724	.7092
1-3	.8755	.3127	.2014	.2699
1-4	1.2829	.1179	.6053	.0873
1-5	2.2693	.0978	.6157	.0856
1-6	2.6962	.0451	1.3901	.0323
1-7	3.3565	.0304	1.6867	.0221
1-8	4.3778	.0251	1.8039	.0199
1-9	6.0027	.0236	1.7561	.0205

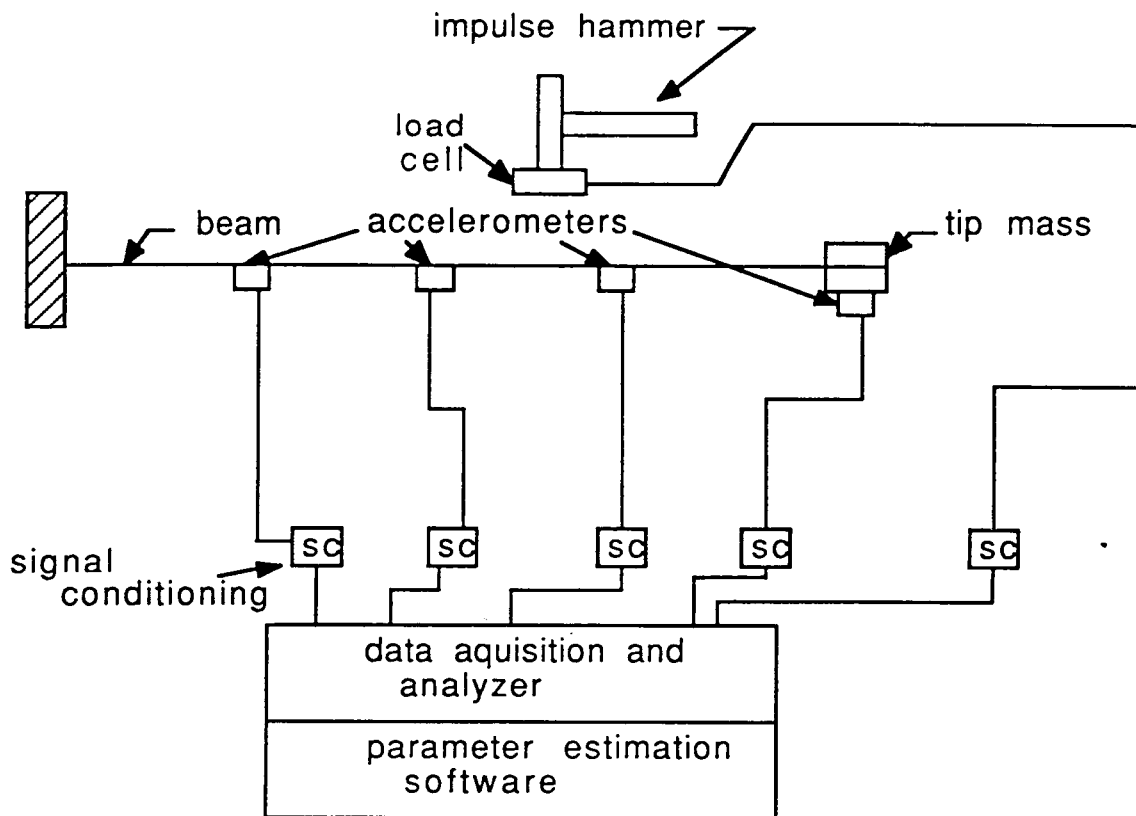


Figure 1. Schematic of test configuration.

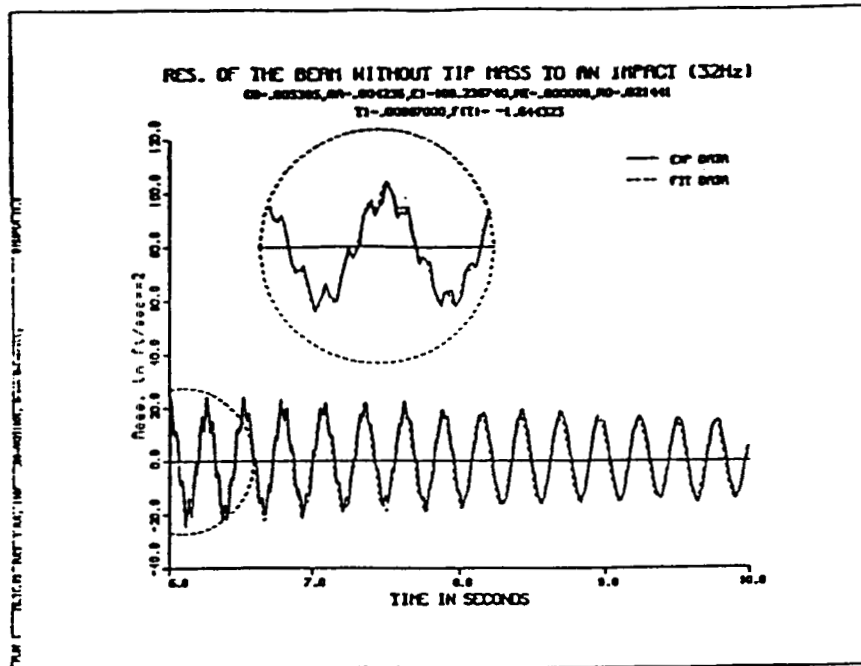


Figure 2. A comparison of the experimentally measured time response and model using q_1 .

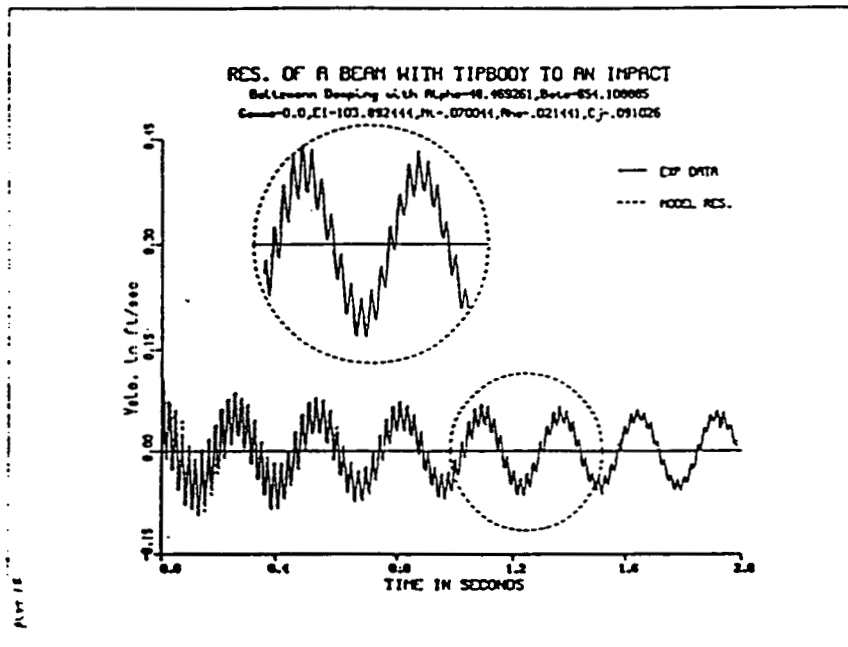


Figure 3. A comparison of the experimentally measured time response and model using q_2 .

ORIGINAL PAGE IS
 OF POOR QUALITY

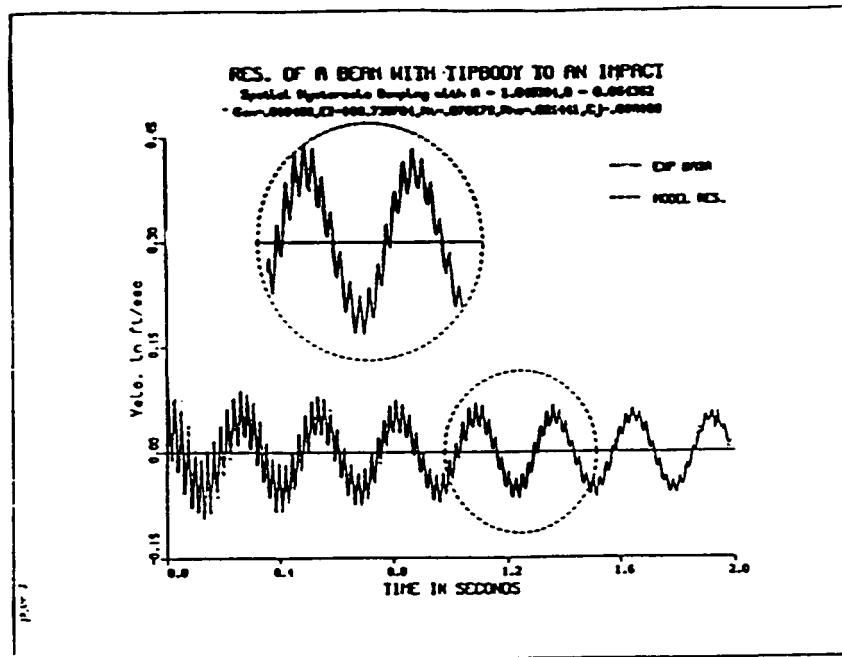


Figure 4. A comparison of the experimentally measured time response and using model q_3 .

ORIGINAL FILED IN
 OF POOR QUALITY



Report Documentation Page

1. Report No. NASA CR-181904 ICASE Report No. 89-64		2. Government Accession No.		3. Recipient's Catalog No.	
4. Title and Subtitle ON DAMPING MECHANISMS IN BEAMS				5. Report Date September 1989	
				6. Performing Organization Code	
7. Author(s) H. T. Banks D. J. Inman				8. Performing Organization Report No. 89-64	
				10. Work Unit No. 505-90-21-01	
9. Performing Organization Name and Address Institute for Computer Applications in Science and Engineering Mail Stop 132C, NASA Langley Research Center Hampton, VA 23665-5225				11. Contract or Grant No. NAS1-18107 NAS1-18605	
				13. Type of Report and Period Covered Contractor Report	
12. Sponsoring Agency Name and Address National Aeronautics and Space Administration Langley Research Center Hampton, VA 23665-5225				14. Sponsoring Agency Code	
15. Supplementary Notes Langley Technical Monitor: ASME Journal of Applied Mechanics Richard W. Barnwell Final Report					
16. Abstract <p>A partial differential equation model of a cantilevered beam with a tip mass at its free end is used to study damping in a composite. Four separate damping mechanisms consisting of air damping, strain rate damping, spatial hysteresis and time hysteresis are considered experimentally. Dynamic tests were performed to produce time histories. The time history data is then used along with an approximate model to form a sequence of least squares problems. The solution of the least squares problem yields the estimated damping coefficients. The resulting experimentally determined analytical model is compared with the time histories via numerical simulation of the dynamic response. The procedure suggested here is compared with a standard modal damping ratio model commonly used in experimental modal analysis.</p>					
17. Key Words (Suggested by Author(s)) damping, inverse problems, composite material beams, experimental verification			18. Distribution Statement 64 - Numerical Analysis Unclassified - Unlimited		
19. Security Classif. (of this report) Unclassified		20. Security Classif. (of this page) Unclassified		21. No. of pages 25	22. Price A03